

Scaling of surface wind speed

Thomas M. Over, Department of Geology/Geography, Eastern Illinois University, Charleston, IL 61920 (Email: tmover@eiu.edu)

Paolo D'Odorico, Department of Environmental Sciences, University of Virginia, Charlottesville, VA 22904 (Email: paolo@virginia.edu)

Introduction

Studies of the scaling of surface wind speed have mainly considered power spectra at small time scales where specialized instrumentation such as hot-wire and sonic anemometers are required, i.e., in the turbulent inertial (microscale) range where a power law with exponent $\beta = -5/3$ is expected and has been observed (e.g., Kaimal et al., 1972), and in the turbulent energy production (mesoscale) range where a power law with exponent $\beta = -1$ power law is predicted and observed (e.g., Katul and Chu, 1998, and references therein). In this study, however, we are interested in what can be seen at time scales observable by standard cup anemometers (i.e., at time resolutions of one minute and above, at the upper end of the mesoscale and above). In addition, recently more general analysis and modeling tools for scaling processes have been developed that go beyond the second-order statistics of power spectra and thus give a fuller picture of the wind structure. These have been applied to micro- and mesoscale winds by Lauren et al., 2001. Here these tools are applied to anemometer data with time resolutions of one to five minutes from Lubbock, Texas and Dodge City, Kansas.

Methods

Several two to four week periods of anemometer data from Lubbock, Texas, and Dodge City, Kansas were analyzed. For some selected series, the periods considered and some basic information along with some results are given in Table I.

A multiscaling analysis following Davis et al. (1994) was performed. This consists of the following steps: (1) spectral analysis to identify scaling ranges, (2) singular measure analysis, and (3) structure function analysis. Power law behavior in the power spectrum gives the initial indication of scaling behavior, and the spectral exponent β gives the domain of the process, which is needed for the rest of the analysis.

A singular measure analysis, as we use the term here, consists of computing the moment scaling function $K(q)$, which is given by

$$\langle \varepsilon(\lambda, t)^q \rangle \sim \lambda^{-K(q)}, \quad \lambda_{\min} \leq \lambda \leq \lambda_{\max}, \quad (1)$$

where $\varepsilon(\lambda, t)$ is the singular measure at time t and coarse-grained to resolution λ , $\langle \cdot \rangle$ indicates averaging over all times t , and λ_{\min} and λ_{\max} are the minimum and maximum resolutions, respectively, over which the scaling holds. In practice, $K(q)$ is found by regressing $\log \langle \varepsilon(\lambda, t)^q \rangle$ vs. $-\log \lambda$ for a set of moment orders q , the slope of the regression giving $K(q)$. Note that in

the case of several scaling ranges as are observed here, different λ_{\min} , λ_{\max} , and $K(q)$ apply to each. A special value of $K(q)$ is its derivative at $q = 1$, called C_1 , which gives the co-dimension of the (measure-theoretic) support of the singular measure. Qualitatively, the bigger C_1 is, the more intermittent is the measure.

The moment scaling function $K(q)$ may be used to estimate the parameters of a process called a random cascade which may be used to simulate a singular measure with the desired $K(q)$ function (see, e.g., Tessier et al., 1993; Over and Gupta, 1994).

Singular measures have spectral power law exponents $\beta = -d + K(2)$, thus $-1 < \beta < 0$. Thus if the spectral exponent of some series has the property $\beta < -1$, then the absolute or squared gradients of the series should be analyzed via a singular measure analysis (if $-3 < \beta < -1$), or gradients of gradients for smaller values of β .

The structure function is designed, as the discussion above suggests, to study the fluctuations of a process $\mathcal{G}(t)$. The structure function $\zeta(q)$ is defined as

$$\langle |\Delta \mathcal{G}(\lambda, t)|^q \rangle \sim \lambda^{\zeta(q)}, \quad \lambda_{\min} \leq \lambda \leq \lambda_{\max}, \quad (2)$$

where $\Delta \mathcal{G}(\lambda, t) = \mathcal{G}(t_{i+\lambda}) - \mathcal{G}(t_i)$. So here the resolution λ indicates the separation distance of two values of the process $\mathcal{G}(t)$ rather than a coarse-grained version of it as it does in singular measure analysis. Similar to the case of the computation of $K(q)$, in practice, $\zeta(q)$ is computed by regressing $\log\langle |\Delta \mathcal{G}(\lambda, t)|^q \rangle$ vs. $\log \lambda$. A special value of $\zeta(q)$ is $H_1 = \zeta(1)$ which gives the Hurst exponent H of fractional Brownian motion (fBm). In fact, for fBm with exponent H ($0 < H < 1$), $\zeta(q) = Hq$. For fBm, the power spectrum follows a power law with $\beta = -1 - 2H$, so $0 < H < 1$ implies $-3 < \beta < -1$, thus a Gaussian process with β in this range may be fBm, while if $-1 < \beta < 1$, it could be modeled as the increments of fBm, i.e., fractional Gaussian noise (fGn). Thus if a process has $-1 < \beta < 1$, before computing its structure function, it should be cumulated.

Results

Results of the are given below in Table I. The most significant finding was that most of the series showed a set of three power law scaling ranges in their power spectra, approximately from 1-10, 10-100, and 100-1000 minutes, with β near -1 in the first, $-1 < \beta < 0$ in the second (suggesting the fGn or singular measure domains), and $-3 < \beta < -1$ in the third (suggesting fBm). An example spectrum from the ARS 7/01 series is given in Figure 1. It should be noted further that the ASOS data was originally in knots and were rounded to the nearest knot, which explains the large value of C_1 for the absolute gradient in the highest frequency range.

<p>Table I. Basic information and results regarding wind data and simulations used in this study. All data is from the 10-m anemometer. The ASOS and ARS data are from Lubbock. The TTU-Mesonet site used is at Reese Center.</p>
--

Data Source, Month	Time Res. (min.)	Duration (min.)	Average Speed (m/s)	Scale Range (minutes)	$-\beta$	series H_1	cum. H_1	series C_1	grad. C_1
NWS-ASOS, 9/00	2	16,384	5.04	2-8	0.98	0.22	0.98	0.004	0.26
				8-128	0.71	0.26	0.98	0.004	0.051
				128-1024	2.08	0.24	0.86	0.017	0.066
ARS, 7/01	1	32,768	4.25	1-8	1.24	0.20	0.96	0.007	0.12
				8-128	0.62	0.18	0.95	0.006	0.018
				128-1024	1.81	0.11	0.74	0.017	0.038
TTU 7/01	5	40,960	4.75	5-80	0.79	0.30	0.97	0.005	0.094
				160-640	1.91	0.24	0.76	0.023	0.073
TTU 9/00	5	40,960	4.44	5-80	0.78	0.30	0.98	0.004	0.095
				160-640	2.01	0.32	0.85	0.017	0.066
Results for simulated series:									
fBm, $H=0.3$	1	65,536	0.20	4-2048	1.58	0.33	0.98	0.003	0.010
fGn, $H=0.8$	1	65,536	0.00	4-2048	0.58	0.022	0.75	0.002	0.012

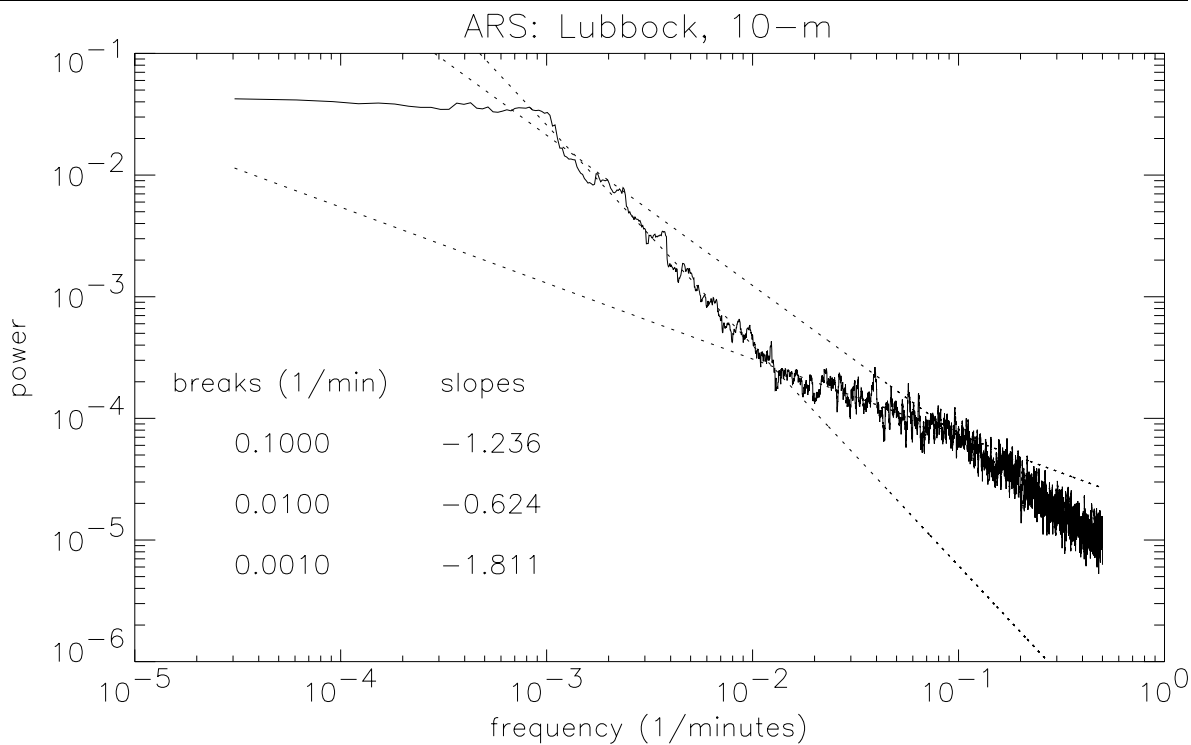


Figure 1. Power spectrum of ARS-Lubbock 10-m wind data for July, 2001.

It generally appears that the singular measure analysis is showing weak intermittency (C_1 near zero), especially if other values of the gradient C_1 are affected by rounding. This would suggest that fGn or fBm (and not a cascade) might be appropriate modeling/downscaling tools, and moment analyses (not shown) suggest the densities (though positively skewed) are not far

from Gaussian, and the complete structure functions (also not shown) are indeed nearly linear. However, the expected behavior of the series and cumulative H_1 values, as may be seen by comparing the simulated fBm and fGn results, is not obtained for the data series. A basic conceptual issue in the use of fBm to model these series would be that they probably should be, on a physical basis, stationary. We note that the value of β near -1 for the highest frequency range matches previous results for the energy production range, though in our case, this value may be affected by the inertia of the instrument. Also, the behavior at the largest scale includes some effects of the diurnal cycle. In summary, while many questions remain to be answered, this analysis has a valuable window on the structure and possible modeling approaches to low frequency surface wind data.

Acknowledgements

This project was supported by Cooperative Agreement No. 2002-35102-11585, award by the U.S. Department of Agriculture.

References

- Davis, A., A. Marshak, W. Wiscombe, and R. Cahalan. 1994. Multifractal characterizations of nonstationary and intermittency in geophysical fields: Observed, retrieved, or simulated. *J. Geophys. Res.* **99**(D4): 8055-8072.
- Kaimal, J. C., J. C. Wyngaard, Y. Izumi, and O. R. Cote. 1972. Spectral characteristics of surface-layer turbulence. *Quart. J. Royal Meteorol. Soc.* **98**: 563-589.
- Katul, G. and C.-R. Chu. 1998. A theoretical and experimental investigation of energy-containing scales in the dynamic sublayer of boundary-layer flows. *Boundary-Layer Meteorol.* **86**: 279-312.
- Lauren, M. K., M. Menabde, and G. L. Austin. 2001. Analysis and simulation of surface-layer winds using multiplicative cascade models with self-similar probability densities. *Boundary-Layer Meteorol.* **100**: 263-286.
- Over, T. M. and V. K. Gupta. 1994. Statistical analysis of mesoscale rainfall: Dependence of a random cascade generator on large-scale forcing. *J. Appl. Meteorol.* **33**(12): 1526-1542.
- Tessier, Y., S. Lovejoy, and D. Schertzer. 1993. Universal multifractals: Theory and observation for rain and clouds. *J. Appl. Meteorol.* **32**(2): 223-250.